Hindawi
Advances in Polymer Technology
Volume 2019, Article ID 8690650, 9 pages
https://doi.org/10.1155/2019/8690650

Research Article

Improvement in Mechanical Properties and Heat Resistance of PLLA-*b*-PEG-*b*-PLLA by Melt Blending with PDLA-*b*-PEG-*b*-PDLA for Potential Use as High-Performance Bioplastics

Supasin Pasee and Yodthong Baimark

Biodegradable Polymers Research Unit, Department of Chemistry and Centre of Excellence for Innovation in Chemistry, Faculty of Science, Mahasarakham University, Mahasarakham 44150, Thailand

Correspondence should be addressed to Yodthong Baimark; yodthong.b@msu.ac.th

Received 29 October 2018; Revised 20 December 2018; Accepted 23 January 2019; Published 24 February 2019

Academic Editor: Lih-sheng Turng

Ecofriendly poly(L-lactide)-*b*-poly(ethylene glycol)-*b*-poly(L-lactide) (PLLA-*b*-PEG-*b*-PLLA) are flexible bioplastics. In this work, the blending of poly(D-lactide)-*b*-poly(ethylene glycol)-*b*-poly(D-lactide) (PDLA-*b*-PEG-*b*-PDLA) with various blend ratios for stereocomplex formation has been proved to be an effective method for improving the mechanical properties and heat resistance of PLLA-*b*-PEG-*b*-PLLA films. The PLLA-*b*-PEG-*b*-PLLA/PDLA-*b*-PEG-*b*-PLDA blend films were prepared by melt blending followed with compression molding. The stereocomplexation of PLLA and PDLA end-blocks were characterized by differential scanning calorimetry and X-ray diffraction (XRD). The content of stereocomplex crystallites of blend films increased with the PDLA-*b*-PEG-*b*-PDLA ratio. From XRD, the blend films exhibited only stereocomplex crystallites. The stress and strain at break of blend films obtained from tensile tests were enhanced by melt blending with the PDLA-*b*-PEG-*b*-PDLA. The heat resistance of blend films determined from testing of dimensional stability to heat and dynamic mechanical analysis were improved with the PDLA-*b*-PEG-*b*-PDLA ratio. The sterecomplex PLLA-*b*-PEG-*b*-PLLA/PDL-*b*-PEG-*b*-PDLA films prepared by melt processing could be used as flexible and good heat-resistance packaging bioplastics.

1. Introduction

In the past few decades, biodegradable bioplastics have been widely developed for use instead of non-biodegradable petroleum-based plastics due to plastic-waste pollution and the implementation of low-carbon environmental protection. Poly(L-lactic acid) or poly(L-lactide) (PLLA) is an important bioplastic that has attracted wide attention due to its nontoxicity, biocompatibility, biodegradability, biorenewability, and good processability [1–3]. PLLA has uses in many fields such as biomedical, food packaging, and agriculture [4–6] but its use in some applications is limited by its low flexibility and poor heat-resistance [7, 8].

Stereocomplex polylactides (scPLA) can be formed by blending between PLLA and poly(D-lactide) (PDLA) that had stronger interactions in the stereocomplex crystallites than the homocrystallites of PLLA and PDLA [9]. This induces higher melting-temperatures (approximately 210–240°C) and faster crystallization speed than the PLLA thereby enhancing the mechanical properties, heat-resistance, and hydrolysis-resistance of scPLA [10, 11]. The high heat-resistant scPLA is appropriate for some applications such as hot-fill packaging, heat-treatment packaging, and microwave applications. However, the glass transition temperature (T_g) of scPLAs was still similar to the PLLA (approximately 60°C). The brittle character of scPLA is still limiting in some applications.

High molecular-weight PLLA-*b*-poly(ethylene glycol)-*b*-PLLA (PLLA-PEG-PLLA) were more flexible than the PLLA because of flexible PEG middle-blocks enhanced plasticizing

effect that decreased the T_g of the PLLA end-blocks [12, 13]. However the heat-resistance of PLLA-PEG-PLLA was still low. In recent years, PLLA has been blended with PDLA-PEG-PDLA for improving the flexibility of the obtained stereocomplex PLLA/PDLA-PEG-PDLA [14–20]. Low-molecular-weight PLLA-PEG-PLLA/PDLA-PEG-PDLA blends were prepared as hydrogels [21–24] and micelles [25, 26] for use as drug delivery carriers. However, the preparation of high-molecular-weight stereocomplex PLLA-PEG-PLLA/PDLA-PEG-PDLA has been scarcely published [27]. The latter work was concerned scPLAs with asymmetric blend ratio. The stereocomplexation of PLLA/PDLA end-blocks and plasticization effect of PEG middle-blocks exhibited better tensile strength, elongation at break, and heat resistance than the PLLA-PEG-PLLA. The melt-blended PLLA-PEG-PLLA/PDLA-PEG-PDLA with various blend ratios has not been reported so far.

All the high-molecular-weight stereocomplex PLLA/PDLA-PEG-PDLA and PLLA-PEG-PLLA/PDLA-PEG-PDLA were prepared by solution blending [14–20, 27]. However the fabrication of scPLA by melt processing is very interesting because of its possible use in industrial-scale applications. The stereocomplexation, mechanical properties, and heat resistance of melt-processed scPLAs need to be better understood for use in practical applications. Therefore in this work, the PLLA-PEG-PLLA/PDLA-PEG-PDLA blend films were prepared by melt blending before compression molding to investigate the influence of blend ratio on their stereocomplexation, mechanical properties, and heat resistance.

2. Materials and Methods

2.1. Materials. L-Lactic acid (L-form optical purity > 95%, 88 %wt, Purac, Thailand) and D-lactic acid (D-form optical purity > 99%, 80 %wt, Haihang Industry (Jinan) Co., Ltd., China) were used as monomer pre-cursors for synthesizing L-lactide (LLA) and D-lactide (DLA) monomers, respectively, by direct polycondensation (step 1) of lactic acid at 180°C for 4.0 h followed with thermal depolymerisation (step 2) under reduced pressure at 10 mmHg of low-molecular-weight poly(lactic acid) at 240°C for 2.0 h. Zinc oxide (99%, Ajax Finechem, Australia) and Stannous octoate ($Sn(Oct)_2$, 95%, Sigma, Switzerland) were used as catalysts in steps 1 and 2, respectively [12]. These crude monomers were purified by recrystallization four times from ethyl acetate before drying in a vacuum oven at 50°C for 24 h. Poly(ethylene glycol) (PEG) with molecular weight of 20,000 g/mol (Sigma, USA) was dried in a vacuum oven at 50°C for 24 h before use.

2.2. Synthesis and Characterization of PLLA-PEG-PLLA and PDLA-PEG-PDLA. The PLLA-PEG-PLLA and PDLA-PEG-PDLA were synthesized by ring-opening polymerization in bulk at 165°C under a nitrogen atmosphere for 6 h using 0.075 mol% $Sn(Oct)_2$ as a catalyst. PEG was used as an initiator. Feed molecular-weights of both the PLLA-PEG-PLLA and the PDLA-PEG-PDLA were calculated based on lactide/PEG feed ratio of 5/1 (w/w) and molecular weight of PEG (20,000 g/mol) that were approximately 120,000 g/mol. The obtained copolymers were granulated before drying in a vacuum oven at 110°C for 3 h to remove any unreacted lactide.

PLLA-PEG-PLLA and PDLA-PEG-PDLA were characterized by polarimetry (Bellingham and Stanley ADP220), gel permeation chromatography (GPC, Waters e2695 separations module), and differential scanning calorimetry (DSC, Perkin-Elmer Pyris Diamond). The characteristics of PLLA-PEG-PLLA and PDLA-EPG-PDLA are summarized in Table 1. The unreacted lactide of copolymers was determined by ^{1}H-NMR. The residue of unreacted lactide of both the PLLA-PEG-PLLA and the PDLA-PEG-PDLA was determined from methine protons of reacted lactide units (δ = 5.15 ppm) and unreacted lactide units (δ = 5.05 ppm) [12] that were less than 1.0 %wt.

2.3. Preparation of PLLA-PEG-PLLA/PDLA-PEG-PDLA Blends. PLLA-PEG-PLLA and PDLA-PEG-PDLA were dried in a vacuum oven at 50°C overnight before melt blending using an internal mixer (HAAKE Polylab OS Rheomix) at 200°C for 4 min with a rotor speed of 100 rpm. The powder solids of the blends were formed when the blending temperature was lower than 200°C [29, 30]. The effects of PLLA-PEG-PLLA/PDLA-PEG-PDLA blend ratios (100/0, 90/10, 80/20, 70/30, 60/40, and 50/50 by weight) were investigated. The obtained blends were granulated before drying in a vacuum oven at 50°C overnight before characterization and compression molding.

The compressed PLLA-PEG-PLLA and blend films were prepared using an Auto CH Carver laboratory press at 240°C without any compression force for 1.0 min and with a 5.0 ton compression force for 1.0 min before cooling to room temperature. The film thicknesses were in ranges 0.20–0.25 mm. The obtained films were kept at room temperature for 24 h before characterization.

2.4. Characterization of PLLA-PEG-PLLA/PDLA-PEG-PDLA Blends. The thermal transition behaviours of the blends were investigated using a Perkin-Elmer Pyris Diamond DSC under a nitrogen flow. For DSC, samples of 3–5 mg in weight were held at 250°C for 3 min to remove thermal history. Then, the samples were quenched to 0°C according to the DSC instrument's own default cooling mode before heating from 0 to 250°C at 10°C/min. For cooling DSC thermograms, the sample was held at 250°C for 3 min to remove thermal history before cooling to 0°C at a rate of 10°C/min.

The degrees of crystallinity from DSC ($X_{c,DSC}$) of homocrystallites (hc-$X_{c,DSC}$) and stereocomplex crystallites (sc-$X_{c,DSC}$) were determined from DSC heating scan using (1) and (2), respectively. Percentage of stereocomplexation (SC) was calculated from (3).

$$\text{hc-}X_{c,DSC}\,(\%) = \left[\frac{(\text{hc-}\Delta H_m - \Delta H_{cc})}{(93 \times W_{PLA})}\right] \times 100 \quad (1)$$

$$\text{sc-}X_{c,DSC}\,(\%) = \left[\frac{(\text{sc-}\Delta H_m - \Delta H_{cc})}{(142 \times W_{PLA})}\right] \times 100 \quad (2)$$

Table 1: Characteristics of PLLA-PEG-PLLA and PDLA-PEG-PDLA.

PLA-PEG-PLA	$[\alpha]^a$ (deg.mL.g^{-1}.dm^{-1})	$M_n{}^b$ (g/mol)	$Đ^b$	$T_g{}^c$ (°C)	$T_m{}^c$ (°C)
PLLA-PEG-PLLA	−122.3	90,000	2.8	31	171
PDLA-PEG-PDLA	+121.5	85,400	2.1	29	170

[a] $[\alpha]$ (specific optical rotation) determined by polarimetry using chloroform as the solvent at 25°C with a wavelength of 589 nm [28].
[b] M_n (number-averaged molecular weight) and dispersity index (Đ) measured by GPC using tetrahydrofuran as the eluent at 40°C.
[c] glass transition temperature (T_g) and melting temperature (T_m) measured by DSC (samples were melted at 200°C for 3 min and cooled to 0°C before scan from 0 to 200°C at 10°C/min under N_2 flow).

$$\text{SC}\,(\%) = \left[\frac{\text{sc-}X_{c,\text{DSC}}}{\left(\text{hc-}X_{c,\text{DSC}} + \text{sc-}X_{c,\text{DSC}}\right)}\right] \times 100 \quad (3)$$

where hc-ΔH_m and sc-ΔH_m were melting enthalpies of homo- and stereocomplex crystallites, respectively. ΔH_{cc} was cold-crystallization enthalpy. Melting enthalpies for hc-$X_{c,\text{DSC}}$ and sc-$X_{c,\text{DSC}}$ = 100% were 93 and 142 J/g, respectively [31]. The weight fraction of the PLA end-blocks (W_{PLA}) was calculated from mole ratio of lactide:ethylene oxide obtained from ^{1}H-NMR and weight of each repeating unit [12] that was 0.83 for both the PLLA-PEG-PLLA and the PDLA-PEG-PDLA.

The crystalline structures of compressed films were measured using a Bruker D8 Advance wide-angle X-ray diffractometer (XRD) at 25°C with CuKα radiation at 40 kV and 40 mA. For XRD, a scan speed of 3°/min was used to determine the crystalline structures. The degrees of crystallinity from XRD ($X_{c,\text{XRD}}$) for homocrystallites (hc-$X_{c,\text{XRD}}$) and stereocomplex crystallites (sc-$X_{c,\text{XRD}}$) of the scPLA films were calculated by using the following, respectively:

$$\text{hc-}X_{c,\text{XRD}}\,(\%) = \frac{S_{hc}}{\left(S_{hc} + S_{sc} + S_a\right)} \times 100 \quad (4)$$

$$\text{sc-}X_{c,\text{XRD}}\,(\%) = \frac{S_{sc}}{\left(S_{hc} + S_{sc} + S_a\right)} \times 100 \quad (5)$$

where S_{hc}, S_{sc}, and S_a were the diffraction peak-areas of homo- and stereocomplex crystallites as well as amorphous hump region, respectively.

The tensile properties of compressed films were determined using a Lloyds LRX+ universal mechanical tester at 25°C and 65% relative humidity. The films (100 × 10 mm) were tested with a gauge length of 50 mm and a crosshead speed of 50 mm/min according to ASTM D882. The tensile properties were averaged from at least five experiments for each sample.

The dimensional stability to heat of compressed scPLA films was tested in an air oven at 80°C for 30 sec under a 200 g load. Initial length of film samples was 20.0 mm. The dimensional stability was calculated by [32]

$$\text{Dimensional stability}\,(\%) = \left[\frac{\text{initial length (mm)}}{\text{final length (mm)}}\right] \times 100 \quad (6)$$

The thermomechanical properties of compressed films measuring 5 × 20 × 0.2 mm in size were investigated with a TA Instrument Q800 dynamic mechanical analyzer (DMA) in a multifrequency strain mode. For DMA analysis, the film samples were heated from 30 to 150°C at the rate of 2°C/min. The scan amplitude was set to be 10 μm and the scanning frequency was 1 Hz.

3. Results and Discussion

3.1. Stereocomplexation. The stereocomplexation between PLLA and PDLA end-blocks of the blends was investigated from DSC heating thermograms as shown in Figure 1. The DSC results are summarized in Table 2. The T_g of the blends were in range 27–29°C. The flexible PEG middle-blocks acted as plasticizers to decrease the T_g of the PLA end-blocks [12, 13]. The stereocomplexation of PLLA and PDLA end-blocks did not affect glass-transition behaviors of the blends.

The PLLA-PEG-PLLA had only a homocrystalline melting peak at 169°C, while the blends had both melting peaks of homocrystallites (hc-T_m) and stereocomplex crystallites (sc-T_m) in the ranges 161–168°C and 216–218°C, respectively. That there were no peaks of cold crystallization suggested that crystallization completed during the quenching process in the DSC method. As shown in Table 2, a large decrease in hc-$X_{c,\text{DSC}}$ and considerable increase in sc-$X_{c,\text{DSC}}$ steadily with increasing PDLA-PEG-PDLA ratio from 0 to 50 wt% were observed. The %SC increased with the PDLA-PEG-PDLA ratio. The higher PDLA-PEG-PDLA ratio gave larger PDLA fraction for stereocomplex formation with the PLLA end-blocks of PLLA-PEG-PLLA.

Figure 2 shows DSC cooling thermograms of the PLLA-PEG-PLLA and blends, after being melted at 250°C. The PLLA-PEG-PLLA had crystallizing temperature (T_c) at 105°C with an enthapy of crystallization (ΔH_c) of 27.4 J/g. The flexible PEG middle-blocks enhanced plasticizing effect for homo-crystallization of PLLA end-blocks during DSC cooling scan. The 90/10 blend exhibited T_c at 84°C that is lower than the pure PLLA-PEG-PLLA. However, the T_c and ΔH_c values of the blends significantly increased with increasing of the PDLA-PEG-PDLA ratio. This suggests the crystallization of the blends was accelerated during the DSC cooling scan by increasing the PDLA-PEG-PDLA ratio. The results could be explained by the crystallization of stereocomplex crystallites of PLA being faster than that of the homocrystallites [33].

The crystalline structures of the PLLA-PEG-PLLA and blend films were determined from XRD patterns as presented in Figure 3. The PLLA-PEG-PLLA film exhibited a diffraction peak at 17° attributed to homocrystalline structure of polylactide matrix [12], while all the blend films showed weak diffraction-peaks at 12°, 21°, and 24° ascribed to

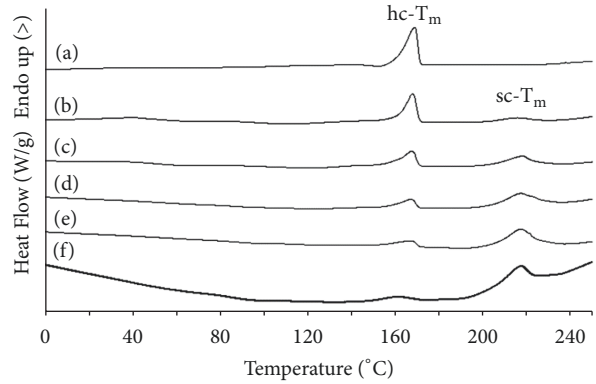

Figure 1: DSC heating thermograms of blends with PLLA-PEG-PLLA/PDLA-PEG-PDLA ratios of (a) 100/0, (b) 90/10, (c) 80/20, (d) 70/30, (e) 60/40, and (f) 50/50 (w/w) (hc-T_m and sc-T_m peaks as shown).

Table 2: DSC results of PLLA-PEG-PLLA/PDLA-PEG-PDLA blends.

PLLA-PEG-PLLA/PDLA-PEG-PDLA (w/w)	hc-T_m (°C)	sc-T_m (°C)	hc-ΔH_m (J/g)	sc-ΔH_m (J/g)	hc-$X_{c,DSC}$ (%)[a]	sc-$X_{c,DSC}$ (%)[b]	SC (%)[c]
100/0	169	-	44.9	-	58.1	-	-
90/10	168	216	30.7	7.6	39.8	6.5	14.0
80/20	168	218	21.0	20.0	27.2	17.0	43.4
70/30	167	216	12.6	27.4	16.3	23.2	58.7
60/40	167	217	10.5	40.3	13.6	34.2	71.6
50/50	161	217	7.7	41.6	10.0	35.2	77.9

[a]calculated from (1).
[b]calculated from (2).
[c]calculated from (3).

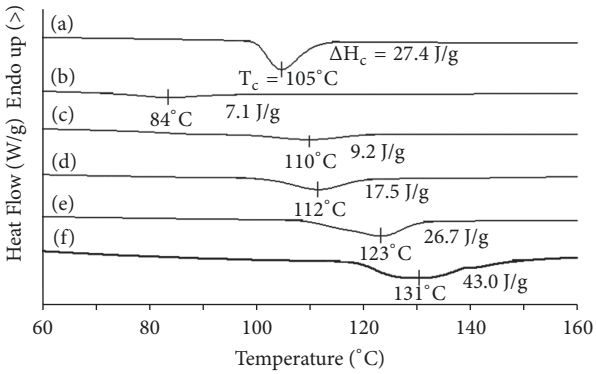

Figure 2: DSC cooling thermograms of blends with PLLA-PEG-PLLA/PDLA-PEG-PDLA ratios of (a) 100/0, (b) 90/10, (c) 80/20, (d) 70/30, (e) 60/40, and (f) 50/50 (w/w) (T_c peaks and ΔH_c values as shown).

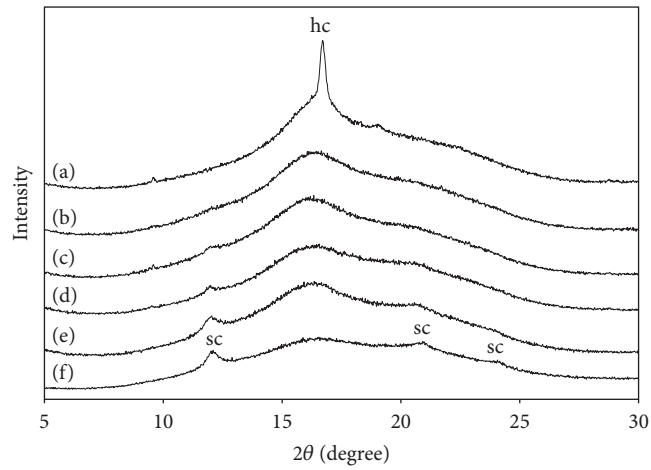

Figure 3: XRD patterns of blend films with PLLA-PEG-PLLA/PDLA-PEG-PDLA ratios of (a) 100/0, (b) 90/10, (c) 80/20, (d) 70/30, (e) 60/40, and (f) 50/50 (w/w).

stereocomplex-crystalline structure [27, 34]. The hc-$X_{c,XRD}$ of PLLA-PEG-PLLA film and sc-$X_{c,XRD}$ of blend films calculated from (4) and (5), respectively, are summarized in Table 3. The sc-$X_{c,XRD}$ of blend films increased with the PDLA-PEG-PDLA ratio. The hc-$X_{c,XRD}$ and sc-$X_{c,XRD}$ values in Table 3 were lower than the hc-$X_{c,DSC}$ and sc-$X_{c,DSC}$ values in Table 2. This may be related to the easier mobility of the copolymer chains, having occurred during the quenching process, without compression forces in the DSC

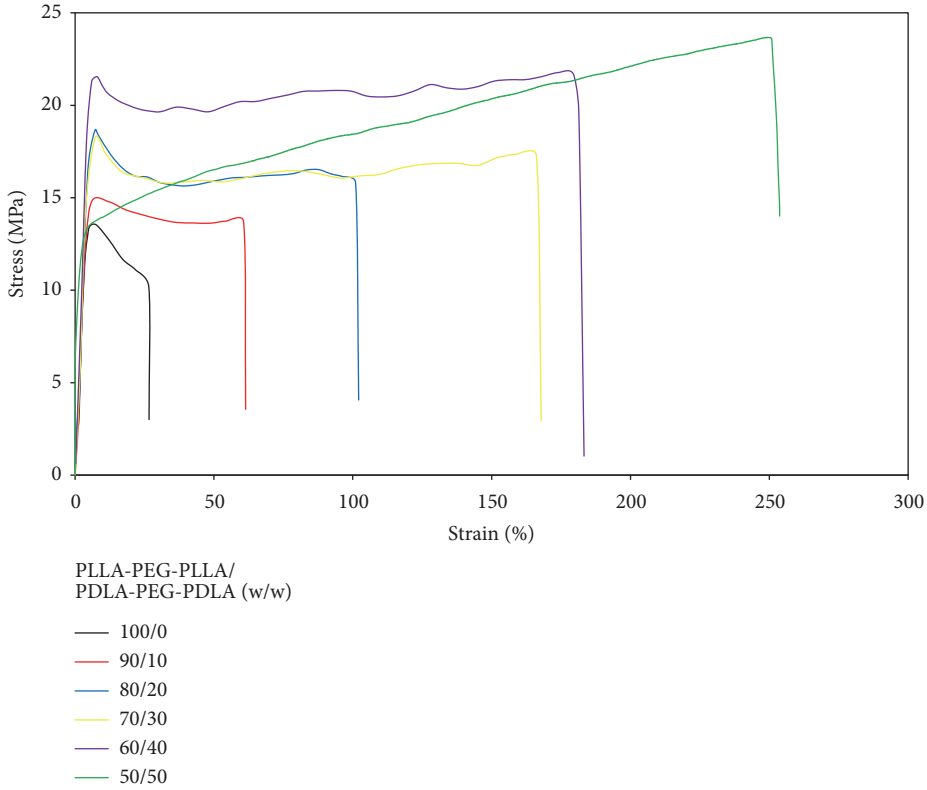

Figure 4: Tensile curves of PLLA-PEG-PLLA/PDLA-PEG-PDLA blend films.

Table 3: XRD results of PLLA-PEG-PLLA/PDLA-PEG-PDLA blend films.

PLLA-PEG-PLLA/PDLA-PEG-PDLA (w/w)	hc-$X_{c,XRD}$ (%)[a]	sc-$X_{c,XRD}$ (%)[b]
100/0	7.84	-
90/10	-	1.94
80/20	-	2.76
70/30	-	3.81
60/40	-	4.72
50/50	-	8.99

[a]calculated from (3).
[b]calculated from (4).

method to enhance more crystallisation of PLA end-blocks. In addition, some disagreements among the quantitative results of the crystallinity by different measurement methods are frequently encountered.

3.2. Tensile Properties. Figure 4 shows selected tensile curves of PLLA-PEG-PLLA and blend films. All the films had a yield point indicating the films were flexible except the 50/50 blend film. The flexible PEG middle-blocks enhanced the plasticizing effect of the polylactide end-blocks [12, 13]. The stress at yield of films increased with the PDLA-PEG-PDLA ratio. The more interactions between PLLA-PEG-PLLA and PDLA-PEG-PDLA in an amorphous phases of the 50/50 blend film might be suppressed the yield effect [27]. The averaged tensile properties including stress and strain at break as well as Young's modulus are clearly compared in Figure 5. The blend films showed higher stress and strain at break than the PLLA-PEG-PLLA film. The stress and strain at break of the blend films increased as the PDLA-PEG-PDLA ratio increased. The results suggested that stereocomplexation between PLLA-PEG-PLLA and PDLA-PEG-PDLA of the blend films improved their tensile properties. The stereocomplex crystallites of PLLA/PDLA end-blocks had better tensile strength than the homocrystallites of PLLA and PDLA end-blocks due to stronger intermolecular forces in the stereocomplex crystallites [9]. The stereocomplex crystallites also acted as physical crosslinkers of PLLA-PEG-PLLA and PDLA-PEG-PDLA chains in film matrix to increased extensibility of the blend films [35, 36]. In addition, the tensile stress at break of the 50/50 melt-blend film (21 MPa) in this work was lower than the 50/50 solution-blend film (~40 MPa) [27]. This may be due to thermal degradation and chain scission during the melt blending. Initial Young's modulus of PLLA-PEG-PLLA and blend films were in ranges 567–640 MPa. That it did not significantly change with the PDLA-PEG-PDLA ratio indicated that the stiffness of the PLLA-PEG-PLLA and blend films was similar. This may be due to the T_g of these films being similar (27–29°C) and their degrees of crystallinity from XRD being low.

3.3. Heat Resistance. The dimensional stability to heat of film samples was determined at 80°C for 30 sec under 200 g load

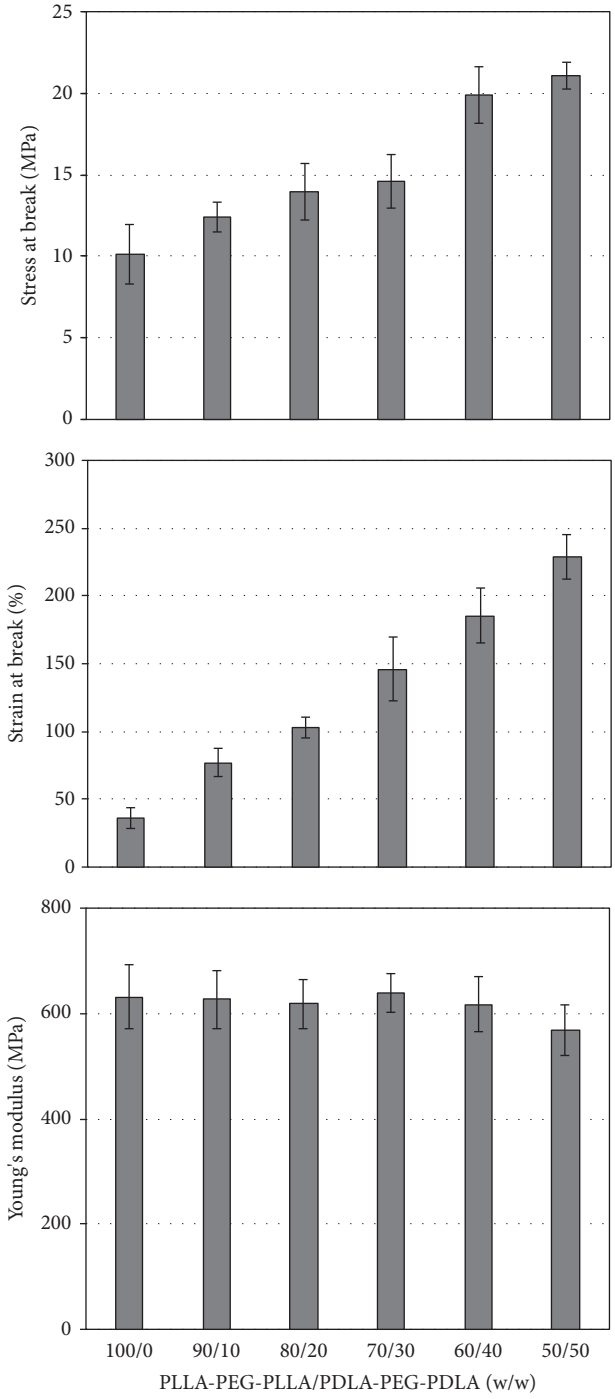

Figure 5: Tensile properties of PLLA-PEG-PLLA/PDLA-PEG-PDLA blend films.

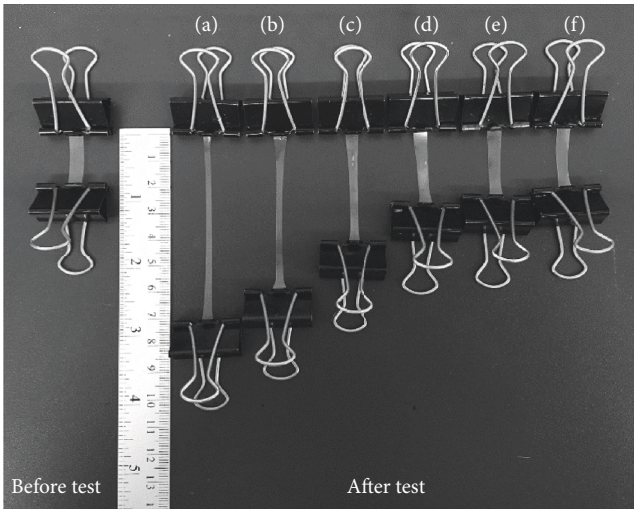

Figure 6: Dimensional stability to heat at 80°C for 30 sec under 200 g load of blend films with PLLA-PEG-PLLA/PDLA-PEG-PDLA ratios of (a) 100/0, (b) 90/10, (c) 80/20, (d) 70/30, (e) 60/40, and (f) 50/50 (w/w).

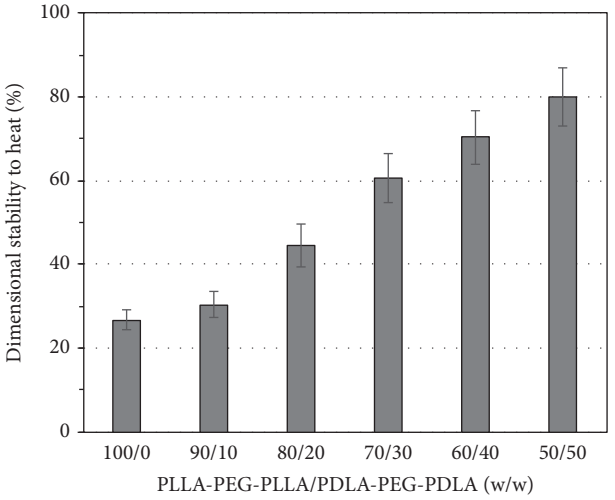

Figure 7: Dimensional stability to heat of PLLA-PEG-PLLA/PDLA-PEG-PDLA blend films.

to study heat resistance of the films. Figure 6 illustrates PLLA-PEG-PLLA and blend films before and after testing. The PLLA-PEG-PLLA film showed the longest film-extension after test [Figure 6(a)]. The film extension decreased when the PDLA-PEG-PDLA was blended and the PDLA-PEG-PDLA ratio was increased.

The heat resistance of the films was compared from the %dimensional stability to heat calculated from (6) that is shown in Figure 7. The %dimensional stability to heat of the films was directly related to the heat resistance that steadily increased with the PDLA-PEG-PDLA ratio. The results suggested that the stereocomplexation of PLLA-PEG-PLLA/PDLA-PEG-PDLA blends improved the heat resistance of the blend films.

The heat resistance of PLLA and scPLA has been widely investigated by DMA analysis from storage modulus as a function of temperature [37, 38]. The storage modulus of low-crystallinity PLLA dramatically dropped as the temperature passing the T_g region before increasing again due to cold crystallization of PLLA during DMA heating scan. This indicated that the low-crystallinity PLLA had poor heat-resistance [39]. Meanwhile good heat-resistance was obtained when the PLLA had a high degree of crystallinity that

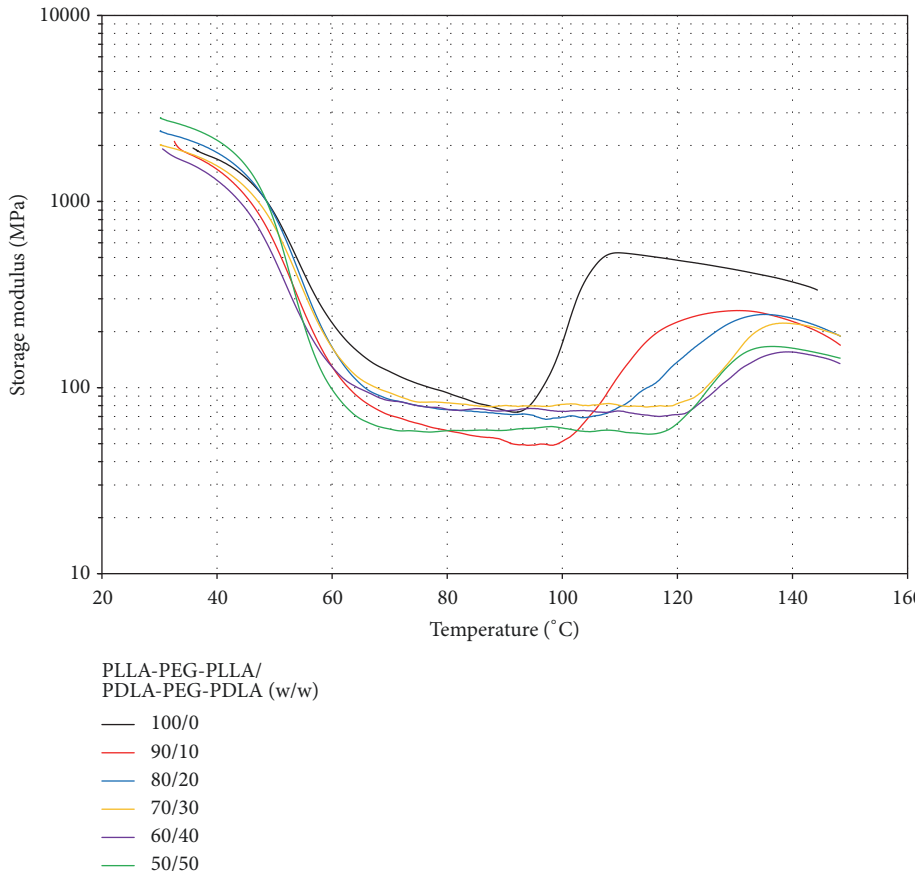

Figure 8: Storage modulus from DMA analysis of PLLA-PEG-PLLA/PDLA-PEG-PDLA blend films.

maintained stiffness of PLLA as it passed through the T_g region [8].

Figure 8 shows storage modulus of film samples from DMA analysis. The storage modulus of PLLA-PEG-PLLA and blend films dramatically dropped with increasing temperature in the range 30–60°C due to rubber-like character and low crystallinity of all the films. This indicates that these films were low heat-resistance. All the films were then extended for the test of dimensional stability to heat. The storage modulus increased again in the range 90–130°C due to cold crystallization of PLA end-blocks. This suggests that the crystallisation of compressed films did not complete. This may be due to the compression forces reducing the chain mobility for crystallisation of PLA end-blocks during the film cooling. However, the cold-crystallization regions of the blend films from DMA analysis were detected at higher temperature than the PLLA-PEG-PLLA film and shifted to higher temperatures as the PDLA-PEG-PDLA ratio increased. This could be explained by the chain mobility of copolymers during cold crystallization in DMA heating scan being restricted by the stronger intermolecular interactions between PLLA and PDLA end-blocks.

In addition, the PLLA-PEG-PLLA film exhibited the largest rising up of storage modulus during cold crystallization (see black line in Figure 8). This curve type indicates that poor heat-resistance of the PLLA-PEG-PLLA film because film stiffness to heat was the lowest [39]. The increases of storage modulus during cold crystallization of the blend films were lower than the PLLA-PEG-PLLA film and steadily decreased as the PDLA-PEG-PDLA ratio increased. The DMA results suggested that the interactions between PLLA and PDLA end-blocks in the amorphous phases of the blend films enhanced its stiffness and heat resistance which supports the results of %dimensional stability to heat in Figure 7. The stronger interactions of PLLA and PDLA end-blocks in the amorphous phases of the blend-film matrix could reduce the film extension during test of dimensional stability to heat.

4. Conclusions

In this work, stereocomplex PLLA-PEG-PLLA/PDLA-PEG-PDLA blend films were prepared by melt blending before compression molding. The blends showed both homo- and stereocomplex crystallites from DSC analysis. The hc-$X_{c,DSC}$ decreased and sc-$X_{c,DSC}$ increased as the PDLA-PEG-PDLA blend ratio increased. The stereocomplexation also enhanced crystallization of PLA matrix. The higher PDLA-PEG-PDLA ratio of the blends induced faster crystallization upon the cooling scan. The XRD results supported the conclusion that the content of stereocomplex crystallites of blend films increased with the PDLA-PEG-PDLA ratio. The mechanical

properties of the blend films were better than the PLLA-PEG-PLLA film and increased with the PDLA-PEG-PDLA ratio. The stereocomplexation between PLLA and PDLA end-blocks improved both stress and strain at break of the blend films. The values of dimensional stability to heat of blend films suggested improvement in their heat resistance that increased with the PDLA-PEG-PDLA ratio. The storage modulus of blend films during cold crystallization determined from DMA indicated that the stronger interactions between PLLA and PDLA end-blocks in the amorphous phases improved the heat resistance. It can be concluded that the PDLA-PEG-PDLA blending can improve mechanical properties and heat resistance of PLLA-PEG-PLLA films for potential use as high-performance bioplastic products.

Data Availability

The data used to support the findings of this study are available from the corresponding author upon request.

Conflicts of Interest

The authors declare that they have no conflicts of interest.

Acknowledgments

This research was financially supported by Mahasarakham University and the Centre of Excellence for Innovation in Chemistry (PERCH-CIC) and the Office of the Higher Education Commission, Ministry of Education, Thailand. The authors gratefully acknowledge Research Professional Development Project under the Science Achievement Scholarship of Thailand (SAST) for providing a scholarship for one of them (SP).

References

[1] E. Castro-Aguirre, R. Auras, S. Selke, M. Rubino, and T. Marsh, "Enhancing the biodegradation rate of poly(lactic acid) films and PLA bio-nanocomposites in simulated composting through bioaugmentation," *Polymer Degradation and Stability*, vol. 154, pp. 46–54, 2018.

[2] D. da Silva, M. Kaduri, M. Poley et al., "Biocompatibility, biodegradation and excretion of polylactic acid (PLA) in medical implants and theranostic systems," *Chemical Engineering Journal*, vol. 340, pp. 9–14, 2018.

[3] S. Chaitanya and I. Singh, "Ecofriendly treatment of aloe vera fibers for PLA based green composites," *International Journal of Precision Engineering and Manufacturing-Green Technology*, vol. 5, no. 1, pp. 143–150, 2018.

[4] J. M. Ugartemendia, A. Larrañaga, H. Amestoy, A. Etxeberria, and J. R. Sarasua, "Tougher biodegradable polylactide system for bone fracture fixations: Miscibility study, phase morphology and mechanical properties," *European Polymer Journal*, vol. 98, pp. 411–419, 2018.

[5] S. Saghazadeh, C. Rinoldi, M. Schot et al., "Drug delivery systems and materials for wound healing applications," *Advanced Drug Delivery Reviews*, vol. 127, pp. 138–166, 2018.

[6] S. Loganathan, J. Jacob, R. B. Valapa, and S. Thomas, "Influence of linear and branched amine functionalization in mesoporous silica on the thermal, mechanical and barrier properties of sustainable poly(lactic acid) biocomposite films," *Polymer Journal*, vol. 148, pp. 149–157, 2018.

[7] A. Nuzzo, S. Coiai, S. C. Carroccio, N. T. Dintcheva, C. Gambarotti, and G. Filippone, "Heat-resistant fully bio-based nanocomposite blends based on poly(lactic acid)," *Macromolecular Materials and Engineering*, vol. 299, no. 1, pp. 31–40, 2014.

[8] X. Zhang, L. Meng, G. Li et al., "Effect of nucleating agents on the crystallization behavior and heat resistance of poly(L-lactide)," *Journal of Applied Polymer Science*, vol. 133, no. 8, Article ID 42999, 2016.

[9] H. Tsuji, "Poly(lactic acid) stereocomplexes: A decade of progress," *Advanced Drug Delivery Reviews*, vol. 107, pp. 97–135, 2016.

[10] E. El-Khodary, Y. Fukui, M. Yamamoto, and H. Yamane, "Effect of the melt-mixing condition on the physical property of poly(L-lactic acid)/poly(D-lactic acid) blends," *Journal of Applied Polymer Science*, vol. 134, no. 44, Article ID 45489, 2017.

[11] Y. Li, Q. Li, G. Yang et al., "Evaluation of thermal resistance and mechanical properties of injected molded stereocomplex of poly(l-lactic acid) and poly(d-lactic acid) with various molecular weights," *Advances in Polymer Technology*, vol. 37, no. 6, pp. 1674–1681, 2018.

[12] Y. Baimark, W. Rungseesantivanon, and N. Prakymoramas, "Improvement in melt flow property and flexibility of poly(L-lactide)-*b*-poly(ethylene glycol)-*b*-poly(L-lactide) by chain extension reaction for potential use as flexible bioplastics," *Materials and Corrosion*, vol. 154, pp. 73–80, 2018.

[13] X. Yun, X. Li, Y. Jin, W. Sun, and T. Dong, "Fast Crystallization and Toughening of Poly(L-lactic acid) by Incorporating with Poly(ethylene glycol) as a Middle Block Chain," *Polymer Science - Series A*, vol. 60, no. 2, pp. 141–155, 2018.

[14] Y. Liu, J. Shao, J. Sun et al., "Improved mechanical and thermal properties of PLLA by solvent blending with PDLA-*b*-PEG-*b*-PDLA," *Polymer Degradation and Stability*, vol. 101, no. 1, pp. 10–17, 2014.

[15] S. Tacha, T. Saelee, W. Khotasen et al., "Stereocomplexation of PLL/PDL-PEG-PDL blends: Effects of blend morphology on film toughness," *European Polymer Journal*, vol. 69, pp. 308–318, 2015.

[16] Z. Jing, X. Shi, G. Zhang, and R. Lei, "Investigation of poly(lactide) stereocomplexation between linear poly(L-lactide) and PDLA-PEG-PDLA tri-block copolymer," *Polymer International*, vol. 64, no. 10, pp. 1399–1407, 2015.

[17] Y. Song, D. Wang, N. Jiang, and Z. Gan, "Role of PEG Segment in Stereocomplex Crystallization for PLLA/PDLA- b -PEG- b -PDLA Blends," *ACS Sustainable Chemistry & Engineering*, vol. 3, no. 7, pp. 1492–1500, 2015.

[18] Z. Li, B. H. Tan, T. Lin, and C. He, "Recent advances in stereocomplexation of enantiomeric PLA-based copolymers and applications," *Progress in Polymer Science*, vol. 62, pp. 22–72, 2016.

[19] Z. Jing, X. Shi, and G. Zhang, "Competitive stereocomplexation and homocrystallization behaviors in the poly(lactide) blends of PLLA and PDLA-PEG-PDLA with controlled block length," *Polymer*, vol. 9, no. 3, p. 107, 2017.

[20] C. Luo, M. Yang, W. Xiao et al., "Relationship between the crystallization behavior of poly(ethylene glycol) and stereocomplex crystallization of poly(L-lactic acid)/poly(D-lactic acid)," *Polymer International*, vol. 67, no. 3, pp. 313–321, 2018.

[21] T. Fujiwara, T. Mukose, T. Yamaoka, H. Yamane, S. Sakurai, and Y. Kimura, "Novel thermo-responsive formation of a hydrogel

by stereo-complexation between PLLA-PEG-PLLa and PDLA-PEG-PDLA block copolymers," *Macromolecular Bioscience*, vol. 1, no. 5, pp. 204–208, 2001.

[22] S. Li, "Bioresorbable Hydrogels Prepared Through Stereocomplexation between Poly(L-lactide) and Poly(D-lactide) Blocks Attached to Poly(ethylene glycol)," *Macromolecular Bioscience*, vol. 3, no. 11, pp. 657–661, 2003.

[23] S. Li and M. Vert, "Synthesis, characterization, and stereocomplex-induced gelation of block copolymers prepared by ring-opening polymerization of L(D)-lactide in the presence of poly(ethylene glycol)," *Macromolecules* , vol. 36, no. 21, pp. 8008–8014, 2003.

[24] S. Li, A. El Ghzaoui, and E. Dewinck, "Rheology and drug release properties of bioresorbable hydrogels prepared from polylactide/poly(ethylene glycol) block copolymers," *Macromolecular Symposia*, vol. 222, pp. 23–35, 2005.

[25] D. G. Abebe and T. Fujiwara, "Controlled thermoresponsive hydrogels by stereocomplexed PLA-PEG-PLA prepared via hybrid micelles of pre-mixed copolymers with different PEG lengths," *Biomacromolecules*, vol. 13, no. 6, pp. 1828–1836, 2012.

[26] C. Feng, M. Piao, and D. Li, "Stereocomplex-reinforced PEGylated polylactide micelle for optimized drug delivery," *Polymer*, vol. 8, no. 4, p. 165, 2016.

[27] L. Han, C. Yu, J. Zhou et al., "Enantiomeric blends of high-molecular-weight poly(lactic acid)/poly(ethylene glycol) triblock copolymers: Enhanced stereocomplexation and thermomechanical properties," *Polymer Journal*, vol. 103, pp. 376–386, 2016.

[28] S. Kumar, N. Bhatnagar, and A. K. Ghosh, "Effect of enantiomeric monomeric unit ratio on thermal and mechanical properties of poly(lactide)," *Polymer Bulletin*, vol. 73, no. 8, pp. 2087–2104, 2016.

[29] Y. Baimark and P. Srihanam, "Influence of chain extender on thermal properties and melt flow index of stereocomplex PLA," *Polymer Testing*, vol. 45, pp. 52–57, 2015.

[30] Y. Srithep, D. Pholharn, L.-S. Turng, and O. Veang-In, "Injection molding and characterization of polylactide stereocomplex," *Polymer Degradation and Stability*, vol. 120, pp. 290–299, 2015.

[31] Y. Xie, X.-R. Lan, R.-Y. Bao et al., "High-performance porous polylactide stereocomplex crystallite scaffolds prepared by solution blending and salt leaching," *Materials Science and Engineering C: Materials for Biological Applications*, vol. 90, pp. 602–609, 2018.

[32] Y. Baimark and S. Kittipoom, "Influence of chain-extension reaction on stereocomplexation, mechanical properties and heat resistance of compressed stereocomplex-polylactide bioplastic films," *Polymer*, vol. 10, no. 11, p. 1218, 2018.

[33] X. Shi, Z. Jing, and G. Zhang, "Influence of PLA stereocomplex crystals and thermal treatment temperature on the rheology and crystallization behavior of asymmetric poly(L-Lactide)/poly(D-lactide) blends," *Journal of Polymer Research*, vol. 25, no. 3, p. 71, 2018.

[34] L. Cui, Y. Wang, Y. Guo et al., "Effects of temperature and external force on the stereocomplex crystallization in poly(lactic acid) blends," *Advances in Polymer Technology*, vol. 37, no. 4, pp. 962–967, 2018.

[35] H. Tsuji, F. Horii, S.-H. Hyon, and Y. Ikada, "Stereocomplex formation between enantiomeric poly(lactic acid)s. 2. stereocomplex formation in concentrated solutions," *Macromolecules*, vol. 24, no. 10, pp. 2719–2724, 1991.

[36] H. Tsuji, S.-H. Hyon, and Y. Ikada, "Stereocomplex formation between enantiomeric poly(lactic acid)s. 3. calorimetric studies on blend films cast from dilute solution," *Macromolecules*, vol. 24, no. 20, pp. 5651–5656, 1991.

[37] W.-J. Si, X.-P. An, J.-B. Zeng, Y.-K. Chen, and Y.-Z. Wang, "Fully bio-based, highly toughened and heat-resistant poly(L-lactide) ternary blends via dynamic vulcanization with poly(D-lactide) and unsaturated bioelastomer," *Science China Materials*, vol. 60, no. 10, pp. 1008–1022, 2017.

[38] K. Masutani, K. Kobayashi, Y. Kimura, and C. W. Lee, "Properties of stereo multi-block polylactides obtained by chain-extension of stereo tri-block polylactides consisting of poly(L-lactide) and poly(D-lactide)," *Journal of Polymer Research*, vol. 25, no. 3, p. 74, 2018.

[39] R. Vadori, A. K. Mohanty, and M. Misra, "The effect of mold temperature on the performance of injection molded Poly(lactic acid)-based bioplastic," *Macromolecular Materials and Engineering*, vol. 298, no. 9, pp. 981–990, 2013.